

NMR and Mössbauer study of spin dynamics and electronic structure of $\text{Fe}_{2+x}\text{V}_{1-x}\text{Al}$ and Fe_2VGa

C. S. Lue, Yang Li, and Joseph H. Ross, Jr.

Department of Physics, Texas A&M University, College Station, TX 77843-4242

George M. Irwin

Department of Chemistry & Physics, Lamar University, Beaumont, TX 77710

(Dated: October 24, 2018)

In order to assess the magnetic ordering process in Fe_2VAl and the related material Fe_2VGa , we have carried out nuclear magnetic resonance (NMR) and Mössbauer studies. ^{27}Al NMR relaxation measurements covered the temperature range 4 – 500 K in $\text{Fe}_{2+x}\text{V}_{1-x}\text{Al}$ samples. We found a peak in the NMR spin-lattice relaxation rate, $^{27}(T_1^{-1})$, corresponding to the magnetic transitions in each of these samples. These peaks appear at 125 K, 17 K, and 165 K for $x = 0.10, 0,$ and -0.05 respectively, and we connect these features with critical slowing down of the localized antisite defects. Mössbauer measurements for Fe_2VAl and Fe_2VGa showed lines with no hyperfine splitting, and isomer shifts nearly identical to those of the corresponding sites in Fe_3Al and Fe_3Ga , respectively. We show that a model in which local band filling leads to magnetic regions in the samples, in addition to the localized antisite defects, can account for the observed magnetic ordering behavior.

I. INTRODUCTION

In recent years, much attention has been focused on inhomogeneous magnetic materials and on their implications in both technological applications and fundamental physics. Granular ferromagnets have been widely investigated since the discovery of giant magnetoresistance (GMR) in these alloys.^{1,2} GMR in granular alloys is associated with the spin-dependent scattering of conduction electrons by disordered magnetic clusters, while in ordered compounds GMR may be associated with scattering from thermal disorder near T_c .³ The Heusler alloys $\text{Fe}_{2+x}\text{V}_{1-x}\text{Al}$ and $\text{Fe}_{2+x}\text{V}_{1-x}\text{Ga}$ are ordered intermetallics which exhibit GMR near T_c ,^{4,5} although in addition to thermal disorder, localized magnetic clusters play a prominent role in these materials, even for the nominally nonmagnetic composition $x = 0$.^{6,7} There has been considerable interest in understanding the role of these clusters for the magnetic transitions, and the unusual electronic behavior associated with these materials.^{8,9,10}

Both Fe_2VAl and Fe_2VGa have been shown to be semimetallic and intrinsically non-magnetic, via electronic structure calculations^{11,12,13,14,15} NMR measurements,^{7,16,17} and optical measurements.^{18,19} These materials adopt the Heusler structure (L2_1 , or cF16 \#225 , AlCu_2Mn type), having a BCC-based lattice in which each Fe ($8c$ position) has four V and four Al or Ga near-neighbors. Complete substitution by Fe on the V sites ($4b$ positions) produces the Fe_3Al structure, DO_3 . Fe_3Al is a metallic ferromagnet in which both Fe sites carry a magnetic moment.²⁰ In $\text{Fe}_{2+x}\text{V}_{1-x}\text{Al}$ T_c goes monotonically to zero as x goes to zero,⁹ although Fe_2VAl exhibits a sample-dependent low-temperature transition which may be residual ferromagnetism^{10,21} or a superparamagnetic freezing temperature.^{7,19} Furthermore in Fe_2VAl and Fe_2VGa localized magnetic

defects have been observed and associated with Fe antisites,^{6,12,15} while there is also evidence for larger magnetic clusters in the materials.^{7,19} No magnetic splitting was observed in Mössbauer studies near the Fe_2VAl composition,^{10,22,23} while the dominance of defects and clusters makes a percolative behavior seem likely.

In order to better understand the local magnetic properties and their changes with composition, we have undertaken NMR and Mössbauer shift studies, providing information about on-site electron densities and the local magnetic configurations of Fe_2VAl , Fe_2VGa , and the mixed composition $\text{Fe}_{2+x}\text{V}_{1-x}\text{Al}$. In previous NMR studies reported by two of us,^{16,24} the lineshapes were shown to be sensitive probes of the magnetic defects in Fe_2VAl and Fe_2VGa , while ^{51}V Korringa relaxation was used to characterize the electronic structure in the region of the semimetallic gap. Here we report measurements of non-Korringa ^{27}Al relaxation behavior near T_c in $\text{Fe}_{2+x}\text{V}_{1-x}\text{Al}$, for compositions bracketing the $x = 0$ phase. We show that relaxation peaks near T_c , together with the lineshapes for these compositions, give a consistent picture of the behavior of antisite defects in this material. The relaxation peaks are due to the critical slowing down of these magnetic defects, and we show that the magnetic defect density tracks the Fe content for the Fe-rich composition. Furthermore, in ^{57}Fe Mössbauer results we identify the isomer shifts for $8c$ sites in Fe_2VAl and Fe_2VGa to differ very little from those of the corresponding Fe sites in Fe_3Al and metastable Fe_3Ga . Thus while the $4b$ -site Fe content changes, the local electronic structure is relatively little affected by the composition change.

II. EXPERIMENT

Samples used for all measurements were a portion of the same ingots used in previous NMR^{7,16,24} and specific heat⁶ measurements. These are polycrystalline samples prepared by arc melting. Ingots were annealed in vacuum at 800 or 1000 °C, then 400 °C, followed by furnace cooling. X-ray powder analysis on all samples showed the expected L2₁ structure, and microprobe analysis confirmed these to be single-phase. Larger lattice constants were found for the non-stoichiometric Fe_{2+x}V_{1-x}Al compositions, similar to those reported in the literature.^{8,9,25}

NMR experiments were performed at fixed field using a 9-T home-built pulse NMR spectrometer described elsewhere.¹⁶ ²⁷Al NMR spectra for all samples were detected near 99 MHz. Ingots were powdered to an approximate 100 - 200 μm particle size. These powders mixed with granular quartz were placed in thin walled plastic vials for 4 to 300 K measurements, and Teflon tubes for high temperature purposes. Both sample holders show no observable ²⁷Al NMR signals.

⁵⁷Fe Mössbauer measurements were obtained using a ⁵⁷Co source in Pd matrix, at ambient temperature, driven in the triangle mode. Results were least-squares fitted using Voigt lineshapes, with shifts referenced to α-Fe. The instrumental broadening was small, as estimated from a Sodium Nitroprusside calibration sample; the reported linewidths were corrected for this term.

III. RESULTS

²⁷Al room-temperature NMR powder patterns for the Fe_{2+x}V_{1-x}Al compounds are shown in Fig. 1, measured by spin-echo integration versus frequency. We found relatively narrow NMR linewidths for Fe₂VAl and Fe_{1.95}V_{1.05}Al, although the latter exhibits an anisotropic line, presumably due to different neighbor configurations in the mixed alloy. The Fe_{2.1}V_{0.9}Al compound, however, shows a significantly broadened ²⁷Al spectrum, which can be attributed to strong local magnetism, corresponding to the bulk magnetism observed for $x > 0$.^{8,9}

The 4a Al sites in Fe₂VAl have cubic site symmetry, and hence no quadrupole broadening for ²⁷Al NMR in the ideal case. However, from pulse-angle studies we determined that the satellite transitions are broadened and made unobservable by random defects, leaving a central line only (1/2 ↔ -1/2 transition). This is typical behavior for dilute alloys,²⁶ even for the small defect densities found in stoichiometric Fe₂VAl. In a previous NMR study⁷ of Fe₂VAl (same ingot as the present $x = 0$ sample), ²⁷Al and ⁵¹V linewidths were found to be identical, and to have a Curie-law temperature dependence with a limiting high-temperature intrinsic width of 3 kHz. The temperature-dependence is characteristic of broadening by local moments, and was shown to be consistent with the presence of magnetic antisite defects.⁷ Clearly for the $x \neq 0$ cases the larger linewidths (Fig. 1) must be

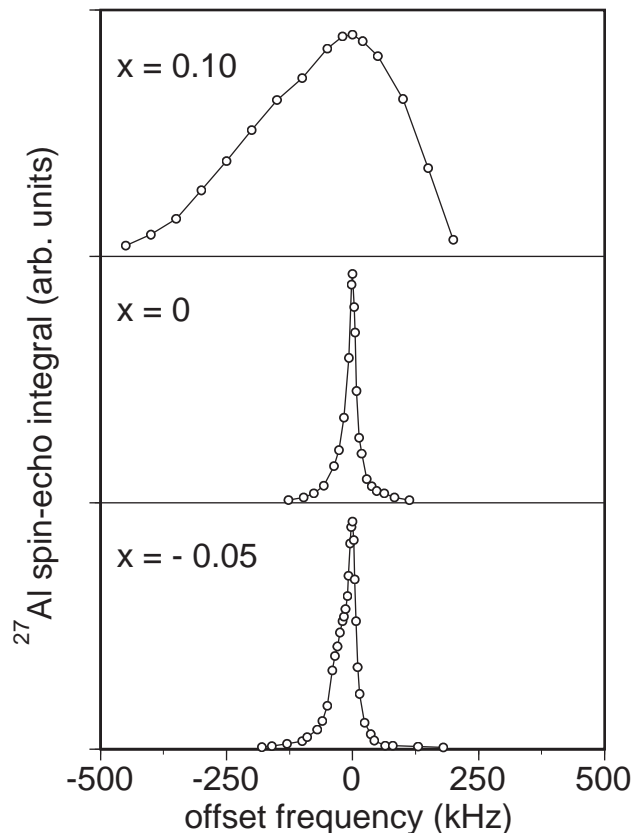


FIG. 1: Room temperature ²⁷Al NMR powder patterns for Fe_{2+x}V_{1-x}Al with $x = 0.10$, 0 , and -0.05 respectively.

caused by inhomogeneous broadening due to the larger defect density in these alloys. From limited temperature-dependence studies we observed the non-stoichiometric samples to have linewidths increasing with decreasing temperature, as would be expected. We measured the spin-echo T_2 and observed a weak temperature increase at low temperatures, to a value of 210 μs at 4 K for $x=0$, consistent with the freezing-in of local fields as the system goes through its spin freezing at low temperatures.⁷ Maksimov et al.¹⁰ have similarly seen a suppression of dynamic relaxation processes at the spin freezing point, in a μSR study.

The antisite-defect dynamics are manifested much more clearly in the ²⁷Al T_1 , rather than the T_2 , and this provides a powerful tool to investigate the spin dynamics. The ⁵¹V T_1 exhibits Korringa behavior at low temperatures, indicating that conduction electrons dominate the relaxation of this nucleus. However, the ²⁷Al T_1 was previously noted to exhibit non-Korringa relaxation in Fe₂VAl.^{16,24} Here we report results of a detailed study showing a clear T_1^{-1} peak for Fe₂VAl, and similar behavior in the $x \neq 0$ materials. Results are shown in Fig. 2 by squares, triangles, and diamonds, for $x = 0.10$, 0 , and -0.05 respectively. Rates were measured by inversion recovery, using the integral of the spin echo fast Fourier transform, irradiating the central portion of the ²⁷Al line.

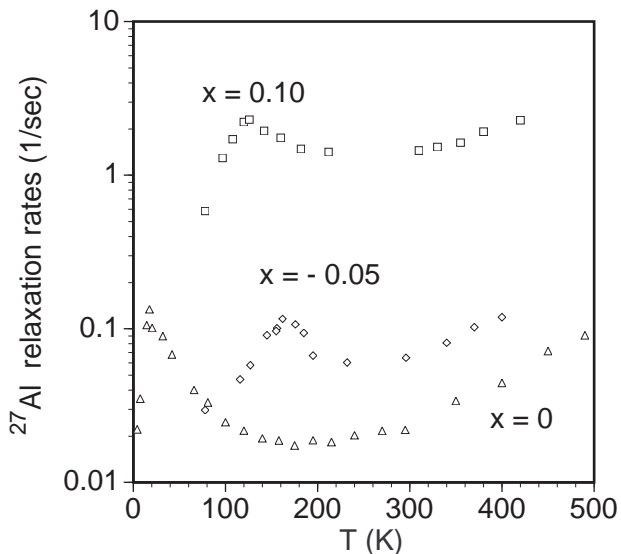


FIG. 2: Temperature dependence of ^{27}Al relaxation rates in $\text{Fe}_{2+x}\text{V}_{1-x}\text{Al}$, indicated by triangles, circles, and diamonds for $x = 0.10$, 0 , and -0.05 respectively.

For the recovery of the central transition, the T_1 's were extracted by fitting to multi-exponential curves²⁷ appropriate for magnetic relaxation of the $I = 5/2$ ^{27}Al central transition.

T_1^{-1} maxima indicate the critical slowing down of the local field fluctuations at the nuclear sites.^{28,29} We find that $^{27}(T_1^{-1})$ passes through a maximum at 125 K, 17 K, and 165 K for $\text{Fe}_{2.1}\text{V}_{0.9}\text{Al}$, Fe_2VAl and $\text{Fe}_{1.95}\text{V}_{1.05}\text{Al}$ respectively. On further cooling, $^{27}(T_1^{-1})$ drops rapidly in all samples. These peaks correspond to susceptibility peaks observed in the same samples.⁷ For $\text{Fe}_{2.1}\text{V}_{0.9}\text{Al}$ this peak corresponds to a ferromagnetic ordering temperature, while for Fe_2VAl the transition may be a superparamagnetic freezing temperature.⁷ It is not entirely clear why no peak was observed for $^{51}(T_1^{-1})$, although for the latter, the presence of d orbitals significantly enhances the Korringa relaxation process, while a small RKKY term might also contribute and be important for ^{51}V .

Room-temperature Mössbauer measurements for both Fe_2VAl and Fe_2VGa yielded single lines, as shown in Fig. 3. The data are shown in the figure, along with the least-squares fitting curves. In both cases, a good fit was obtained using a single Voigt-broadened line. The two linewidths thus determined are identical, and slightly larger than the natural width for Fe. Parameters from these fits are given in Table I. The widths given in the table are excess values over the natural width for Fe. These small widths indicate a relative lack of inhomogeneous broadening, showing these samples to be well-ordered in the Heusler structure, with very similar Fe site occupancies. Also shown in the table are isomer shifts for Fe_3Al and Fe_3Ga , from Lin *et al.*³⁰ and Kawamiya *et al.*³¹, respectively. There have been a number of Mössbauer studies of the stable compound

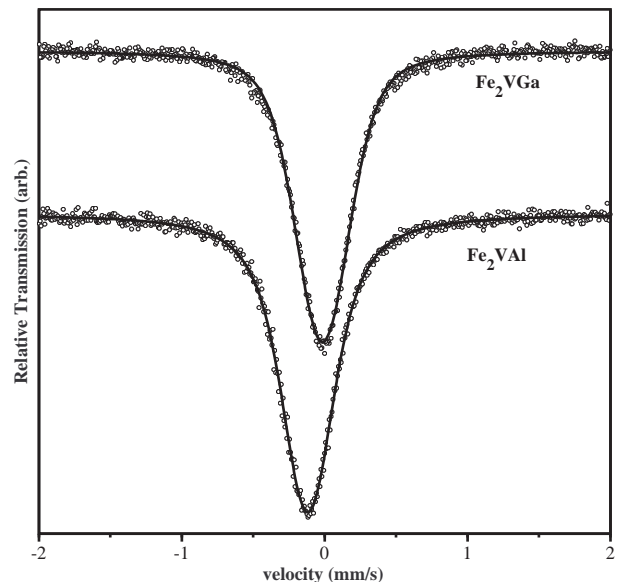


FIG. 3: Room-temperature Mössbauer spectra for Fe_2VAl and Fe_2VGa . Least-squares fits are superposed on the data. Velocities are relative to the source.

TABLE I: Measured Mössbauer isomer shifts and widths, along with NMR Knight shifts and lattice parameters. Room-temperature isomer shifts (δ) and line widths (σ) are listed. Isomer shifts are quoted relative to an α -Fe reference. Vanadium Knight shifts (K_V) are low-temperature values. Wyck-off positions labels are given for the DO_3 lattice (equivalent to the L_{21} labels).

Material	a (nm)	site	δ (mm/s)	σ (mm/s)	K_V (%)
Fe_2VAl	0.576^b	8c	$0.058(5)^a$	$0.054(5)^a$	0.61^b
Fe_3Al		8c	0.05^c		
		4b	0.19^c		
Fe_2VGa	0.577^b	8c	$0.161(5)^a$	$0.054(5)^a$	0.59^b
Fe_3Ga		8c	0.18^d		
		4b	0.28^d		

^aThis work.

^bRef. 7.

^cRef. 30.

^dRef. 31.

Fe_3Al ,^{20,30,32,33} while for Fe_3Ga the DO_3 structure is metastable, and quenched samples were used to obtain the referenced values. Finally, for comparison, values for the vanadium Knight shift and the cubic lattice constant of Fe_2VAl and Fe_2VGa are shown in the table. These values are quite close, indicating the similarity of these two materials.

IV. DISCUSSION

Previously, the temperature dependences of the ^{27}Al and ^{51}V linewidths in Fe_2VAl were fit using the analyt-

ical results of Walstedt and Walker³⁴ for dipolar broadening due to random local-moment spins. Taking the local moments to be antisite defects of $3.7 \mu_B$ as obtained from specific heat measurements,⁶ this fit yielded a defect concentration of $c = 0.0045$,⁷ per formula unit, which compares favorably with the value $c = 0.0037$ obtained from specific heat. In the dilute limit, the lineshape for this mechanism will be Lorentzian, with identical widths for ^{27}Al and ^{51}V , as indeed observed in Fe_2VAL .⁷ These results give confidence that the broadening mechanism and the defect concentration are well understood. Note that several groups have identified the presence of large-moment clusters in addition to the antisite local moments in Fe_2VAL ,^{7,19} however these turn out to have a much smaller contribution to the Fe_2VAL NMR linewidth.⁷

For dipolar broadening in NMR, in the dilute limit one finds that the Lorentzian line has a width proportional to c .³⁴ From the data of Fig. 1 we find that the $x = 0.10$ sample exhibits a half-width 17 times larger than that of the $x = 0$ sample. Nominally this implies an antisite concentration for $x = 0.10$ of $c = 0.077$ per formula unit, and although this value is outside the dilute limit where the analytic expressions are no longer exact, this provides an approximate estimate of the density of local defects. This sample contains $c = 0.10$ excess Fe per formula unit, so the model described here shows that a sizable portion (possibly all) of the excess Fe is distributed as random defects on V sites, rather than clustered within the sample.

NMR spin-lattice relaxation due to an uncorrelated population of local moments has been treated by several authors.^{29,35,36,37,38} If nuclear spin-diffusion is not important, the relaxation function is a stretched exponential, $s(t) \propto \exp - (t/\tau_1)^{1/2}$, due to an inhomogeneous distribution of local relaxation rates. For a concentration n per unit volume of effective moments p , the exponential factor is,³⁶

$$\tau_1^{-1} = 0.84 \frac{p\mu_B\gamma n n}{\sqrt{\omega}} \left(\frac{\omega\tau_c}{1 + \omega^2\tau_c^2} \right)^{1/2}, \quad (1)$$

where ω is the NMR frequency, and a single Debye-type correlation time τ_c has been assumed to apply to the local moments. At a temperature where $\tau_c = \omega$, a maximum occurs in Eq. (1), giving $\tau_1^{-1} = 0.19 \text{ s}^{-1}$ for our $x = 0$ sample, using the values $p = 3.7$ and $n = 7.6 \times 10^{19} \text{ cm}^{-3}$ (corresponding to $c = 0.0037$), values taken from the specific heat measurement⁷ and described above. A distribution of correlation times will give a somewhat lower peak value. In our T_1^{-1} measurements, for each temperature the signal amplitude was measured over one or two decades of recovery time, and a best fit was made to the three-exponential $I = 5/2$ magnetic relaxation function for central transition inversion-recovery.²⁷ For central-transition measurements, the stretched-exponential curve for local-moment relaxation should be convoluted with the same $I = 5/2$ multi-exponential. From numerical plots we found that such a convolution is nearly indistinguishable from the

three-exponential recovery curve if $\tau_1 = T_1$ over about one decade of recovery time. The peak value observed for $x = 0$ (Fig. 2) is $T_1^{-1} = 0.13 \text{ s}^{-1}$, in good agreement with the value 0.19 s^{-1} obtained from the model described here. Therefore, just as for the lineshapes, the density of local moments obtained independently, and attributed to antisite defects, is in good quantitative agreement with the observed $^{27}\text{T}_1^{-1}$ peak value in the $x = 0$ sample.

Local-moment relaxation of this type scales with n (Eq. (1), exact in the limit of dilute moments). From the data in Fig. 2, the peak value of T_1^{-1} is found to be 17 times larger for the $x = 0.10$ sample than for the $x = 0$ sample. This is the same ratio as found for the linewidths, thus giving quantitative consistency with the model, showing that the excess Fe act as local moments fluctuating independently in the paramagnetic regime at this concentration. The peaks observed in T_1^{-1} coincide with maxima in the ac susceptibility,³⁹ and therefore correspond to magnetic transitions in the samples. The relaxation peaks can be attributed to critical slowing down of the local moment dynamics at these transition temperatures. Maxima in the μSR longitudinal relaxation rate were also observed by Maksimov, *et al.*¹⁰ attributed to the same mechanism.

For the $x = -0.05$ sample the density of local moments is smaller than for the $x = 0.10$ sample; this can be seen from both the NMR linewidth and the peak value of $^{27}\text{T}_1^{-1}$. On the other hand, the transition temperature for this sample is the largest of the three. Of course, the local moment density might be expected to be smaller since there is no Fe excess in this sample. Thus, the moment density does not necessarily correlate with T_c in this material. Indeed, as has been pointed out previously,¹⁰ the local moment density is below the percolation limit in all of these samples, and thus it is not sensible that the magnetic transitions are driven solely by the interaction of these moments.

Another feature identified in Fe_2VAL is the presence of a more dilute set of large moments.^{7,19} These were shown previously to induce superparamagnetic behavior in Fe_2VAL ,⁷ although their contribution to the NMR linewidth is small. The spin-lattice relaxation time will also not be affected by these moments, since they will be saturated in the measuring magnetic field. Since no second phase was observed in electron microprobe measurements, we propose that the large moments are ferromagnetic regions in the Heusler lattice having enhanced conduction electron density, perhaps associated with variations in Fe concentration. Indeed, Fe_2VAL is a semimetal, but with increasing x becomes ferromagnetic, its metallic bands becoming occupied.^{9,24} The interaction of locally ferromagnetic regions can lead to superparamagnetic freezing in Fe_2VAL , while with increasing x these regions percolate, leading to ferromagnetic ordering. According to the values obtained earlier,⁷ the 17 K T_1^{-1} peak for $x = 0$ must be due to field polarization of the antisite spins, while the higher-temperature peaks for $x \neq 0$ must be due to antisite defects which are coupled by band

electrons.

With sufficient Fe concentration $\text{Fe}_{2+x}\text{V}_{1-x}\text{Al}$ will approach Fe_3Al , in which the $8c$ sites carry a moment, in addition to the $4b$ sites (antisites for Fe_2VAl).²⁰ Mössbauer measurements give us a measure of the electronic structure changes involved in this behavior. We have found (Table I) that the isomer shift for Fe_2VAl is nearly identical to that of the corresponding $8c$ site in Fe_3Al . A similar result is seen for Fe_2VGa and Fe_3Ga . A large change in average isomer shift was found vs. V substitution by Shobaki *et al.*,²³ but this can be attributed to a change in Fe site occupation. Since the most important contribution to the isomer shift is due to the on-site s -electron concentration, clearly very little electron transfer into s -orbitals is involved in the substitution of Fe for V. We conclude that at least in this regard, the Fe local electronic structure is not substantially changed by the change of its neighbors from V to Fe. We picture the addition of Fe leading to the filling of d -bands in a manner rather like that of a rigid band model.

The isomer shift for Fe_3Ga is significantly different from that of Fe_3Al . This seems surprising given the close similarity of the two materials. For example, the vanadium Knight shifts quoted in Table I are nearly identical, and these measure the orbital susceptibility of the d -bands in the two materials. However, large isomer

shifts have also been observed in Fe_3Ga_4 .⁴⁰ Apparently the larger Ga atom leads to more covalent bonding, thus stabilizing p and d orbitals relative to s .

V. CONCLUSIONS

A measurement of the ^{27}Al NMR lineshapes and spin-lattice relaxation in $\text{Fe}_{2+x}\text{V}_{1-x}\text{Al}$ showed that a consistent measure of the local moment density and dynamics could be obtained. For $x = 0.10$, the local moment density is approximately equal to the excess Fe concentration. This density is below the percolation limit, although the material has a ferromagnetic transition. The development of a metallic band can explain this transition. Mössbauer measurements show that little change in Fe local electronic structure accompanies the change from semimetallic Fe_2VAl to ferromagnetic Fe_3Al , with a similar result found for Fe_2VGa .

Acknowledgments

This work was supported by the Robert A. Welch Foundation, Grant No. A-1526.

-
- ¹ A. E. Berkowitz, J. R. Mitchell, M. J. Carey, A. P. Young, S. Zhang, F. E. Spada, F. T. Parker, A. Hutten, and G. Thomas, *Phys. Rev. Lett.* **68**, 3745 (1992).
 - ² J. Q. Xiao, J. S. Jiang, and C. L. Chien, *Phys. Rev. Lett.* **68**, 3749 (1992).
 - ³ J. M. D. Coey, in *Aspects of Modern Magnetism*, edited by F. C. Pu, Y. J. Wang, and C. H. Shang (World Scientific, 1996), p. 2.
 - ⁴ K. Endo, H. Matsuda, K. Ooiwa, M. Iijima, T. Goto, K. Sato, and I. Umehara, *J. Magn. Magn. Mater.* **177-181**, 1437 (1998).
 - ⁵ H. Matsuda, K. Endo, K. Ooiwa, M. Iijima, Y. Takano, H. Mitamura, T. Goto, M. Tokiyama, and J. Arai, *J. Phys. Soc. Japan* **69**, 1004 (2000).
 - ⁶ C. S. Lue, J. H. Ross, Jr., C. F. Chang, and H. D. Yang, *Phys. Rev. B* **60**, R13941 (1999).
 - ⁷ C. S. Lue, J. H. Ross, Jr., K. D. D. Rathnayaka, D. G. Nangle, S. Y. Wu, and W.-H. Li, *J. Phys.: Condens. Matter* **13**, 1585 (2001).
 - ⁸ Y. Nishino, M. Kato, S. Asano, K. Soda, M. Hayasaki, and U. Mizutani, *Phys. Rev. Lett.* **79**, 1909 (1997).
 - ⁹ M. Kato, Y. Nishino, U. Mizutani, and S. Asano, *J. Phys.: Condens. Matter* **12**, 1769 (2000).
 - ¹⁰ I. Maksimov, D. Baabe, H. H. Klauss, F. J. Litterst, R. Feyerherm, D. M. Többens, A. Matsushita, and S. Stülow, *J. Phys.: Condens. Matter* **13**, 5487 (2001).
 - ¹¹ G. Y. Guo, G. A. Botton, and Y. Nishino, *J. Phys.: Condens. Matter* **10**, L119 (1998).
 - ¹² D. J. Singh and I. I. Mazin, *Phys. Rev. B* **57**, 14352 (1998).
 - ¹³ R. Weht and W. E. Pickett, *Phys. Rev. B* **58**, 6855 (1998).
 - ¹⁴ M. Weinert and R. E. Watson, *Phys. Rev. B* **58**, 9732 (1998).
 - ¹⁵ A. Bansil, S. Kaprzyk, P. E. Mijnders, and J. Tobola, *Phys. Rev. B* **60**, 13396 (1999).
 - ¹⁶ C. S. Lue and J. H. Ross, Jr., *Phys. Rev. B* **58**, 9763 (1998).
 - ¹⁷ In the previous reference, labels on the vertical axis of figure 3(a) were a factor of 10 too small. This does not affect the conclusions of that paper.
 - ¹⁸ H. Okamura, J. Kawahara, T. Nanba, S. Kimura, K. Soda, U. Mizutani, Y. Nishino, M. Kato, I. Shimoyama, H. Miura, et al., *Phys. Rev. Lett.* **84**, 3674 (2000).
 - ¹⁹ Y. Feng, J. Y. Rhee, T. A. Wiener, D. W. Lynch, B. E. Hubbard, A. J. Sievers, D. L. Schlagel, T. A. Lograsso, and L. L. Miller, *Phys. Rev. B* **63**, 165109 (2001).
 - ²⁰ M. B. Stearns, *Phys. Rev.* **168**, 588 (1968).
 - ²¹ A. Matsushita and Y. Yamada, *J. Magn. Magn. Mater.* **196-197**, 669 (1999).
 - ²² E. Popiel, M. Tuszynski, W. Zarek, and T. Rendecki, *J. Less-Common Met.* **146**, 127 (1989).
 - ²³ J. Shobaki, I. A. Al-Omari, M. K. Hasan, K. A. Azez, M.-A. H. Al-Akhras, B. A. Albiss, H. H. Hamdeh, and S. H. Mahmood, *J. Magn. Magn. Mater.* **213**, 51 (2000).
 - ²⁴ C. S. Lue and J. H. Ross, Jr., *Phys. Rev. B* **61**, 9863 (2000).
 - ²⁵ W. Zarek, E. Talik, J. Heimann, M. Kulpa, A. Winiarska, and M. Neumann, *J. Alloys. Comp.* **297**, 53 (2000).
 - ²⁶ O. Kanert and M. Mehring, in *NMR: Basic Principles and Progress*, edited by E. Fluck and R. Kosfeld (Springer-Verlag, New York, 1971), vol. 3, p. 1.
 - ²⁷ A. Narath, *Phys. Rev.* **162**, 320 (1967).
 - ²⁸ T. Moriya, *Spin Fluctuations in Itinerant Electron Magnetism* (Springer-Verlag, 1985).
 - ²⁹ A. Narath, *CRC Crit. Rev. Solid State Sci.* **3**, 1 (1972).

- ³⁰ M.-C. Lin, R. G. Barnes, and D. R. Torgeson, Phys. Rev. B **24**, 3712 (1981).
- ³¹ N. Kawamiya, K. Adachi, and Y. Nakamura, J. Phys. Soc. Japan **33**, 1318 (1972).
- ³² S. B. Raju, J. P. Eymery, and P. Moine, Scr. Metall. **13**, 649 (1979).
- ³³ B. Fultz, Z. Gao, H. H. Hamdeh, and S. A. Oliver, Phys. Rev. B **49**, 6312 (1994).
- ³⁴ R. E. Walstedt and L. R. Walker, Phys. Rev. B **9**, 4857 (1974).
- ³⁵ I. J. Lowe and D. Tse, Phys. Rev. **166**, 279 (1968).
- ³⁶ D. Tse and S. R. Hartmann, Phys. Rev. Lett. **21**, 511 (1968).
- ³⁷ C. C. Sung and L. G. Arnold, Phys. Rev. B **7**, 2095 (1973).
- ³⁸ G. B. Furman, E. M. Kunoff, S. D. Goren, V. Pasquier, and D. Tinetti, Phys. Rev. B **52**, 10182 (1995).
- ³⁹ C. S. Lue, Ph.D. thesis, Texas A&M University (1999).
- ⁴⁰ M. A. Kobeissi, J. A. Hutchings, P. G. Appleyard, M. F. Thomas, and J. G. Booth, J. Phys.: Condens. Matter **11**, 6251 (1999).